ELSEVIER

Journal of Nuclear Materials 307–311 (2002) 514–520

journal of nuclear materials

www.elsevier.com/locate/jnucmat

Modelling of the effect of precipitates on work-hardening, ductility and impact behaviour of ferritic–martensitic Cr steels

D. Preininger *

Forschungszentrum Karlsruhe, Institute for Materials Research I, P.O. Box 3640, D-76021 Karlsruhe, Germany

Abstract

The effect of precipitates on work-hardening, tensile ductility and impact behaviour of carbon and high nitrogen martensitic 7–12Cr as well as particle strengthened ODS-(9–13)Cr steels have been analysed by models. A minimum of work-hardening and uniform strain generally appears around 600 °C at onset of dislocation recovery. Pronounced precipitation by increasing nitrogen and carbon content or additionally of fine Y_2O_3-particles distinctly increases work-hardening and uniform ductility. These, however, decrease with increasing strengthening but do not reach a visible level above 1500 MPa for ODS-steels at 20 °C. Minima of total elongation and fracture strain additionally appear in carbon and nitrogen martensitic steels around 300 °C where dynamic strain ageing occurs. Fracture strain and ductile upper shelf energy of Charpy tests in accordance with model predictions also decrease with increasing yield strength more strongly for ODS-steels due to their enhanced work-hardening and localized deformation. The strength-induced increase of ductile-to-brittle transition temperatures of ODS-steels is comparable to that observed by irradiation defect strengthening.

1. Introduction

Strengthening of ferritic–martensitic chromium steels by small and thermally stable particles is a very useful way to improve creep strength and irradiation resistance by enhanced absorbtion of irradiation-produced defects. Oxide dispersion-strengthened ODS-(9–13)Cr alloys are being developed using powder metallurgy technique for application as fusion structural material which might increase the applicability to higher temperatures of 600/650 °C. However, due to the pronounced strengthening, tensile ductility and impact properties are degraded which could restrict their application as structural materials.

In this paper the effect of precipitates on work-hardening, tensile ductility and impact behaviour of martensitic reduced activation 7–9CrW(Ge)VTa carbon, 12CrMo(W)V(Ti) high nitrogen ($\leqslant 0.2$ wt%) as well as oxide dispersion-strengthened ferritic–martensitic ODS-(9–13)Cr steels have been analysed by deformation and stress-induced fracture models. Particularly the influence of volume fraction and size of carbide/nitride or incoherent Y_2O_3-particles as well as alloy composition are considered. By analysis of experimental results the metallurgical possibilities for the improvement of tensile ductility and impact behaviour at simultaneous high strength are discussed for the reduced activation ODS-steels.

2. Model for the effect of precipitates on work-hardening, tensile ductility and impact behaviour

Work-hardening by strain (ε)-induced dislocation populations with density $\rho(\varepsilon)$ can by usually expressed by $\Delta\sigma_\varepsilon = \alpha\mu bM(\rho)^{1/2}$. Here, $\alpha = 0.1$–0.4 is a strength coefficient, μ the shear modulus, b the Burgers vector

* Tel.: +49-7247 82 3639; fax: +49-7247 82 4567.
E-mail address: dieter.preininger@imf.fzk.de (D. Preininger).

0022-3115/02/$ - see front matter
PII: S0022-3115(02)01210-2

and $M \approx 2.5$–3 the Taylor factor. Dislocation evolution can be well described by the rate equation $\delta\rho/\delta\varepsilon = A - B$ through a balance between dislocation multiplication A, induced by glide and precipitates as well as annihilation B [1]. Dislocation multiplication according to $A = M[1/(b\Lambda) + 8f_v/(bd_p)]$ depends on the mean glide distance of dislocations Λ, and is enhanced by presenting precipitates due to generation of geometrically necessary dislocations dependent on the ratio of volume fraction f_v to mean size d_p of particles. Dislocation annihilation $B = 2RM\rho/b$ otherwise increases with increasing dislocation density ρ and critical distance R below which dislocations of different signs annihilate spontaneously. From this work-hardening model described in [2], the true uniform strain, ε_u, for $\Lambda =$ constant, which is generally applicable for body centered cubic metals below $\approx 0.3T_m$ (melting temperature) is given by the relation

$$\begin{aligned} \varepsilon_u &= -[1/(2R_m)]\ln\{1-\eta_\varepsilon^2\}, \\ \eta_\varepsilon &= \{[1+4R_m(1+R_m)y^2]^{1/2}-1\}/[2(1+R_m)y], \end{aligned} \tag{1}$$

where $y = \Delta\sigma_{\varepsilon,m}/\sigma_y$ describes the ratio of maximum strain hardening ($\varepsilon \to \infty$) and $R_m = RM/b$ the normalized annihilation coefficient. Maximum strain hardening $\Delta\sigma_{\varepsilon,m} = \alpha\mu bM\{[1+8\Lambda f_v/d_p]/(2R\Lambda)\}^{1/2}$ increases with decreasing glide distance Λ and annihilation distance R as well as increasing ratio f_v/d_p of particles. Work-hardening described by the ratio $\eta = \sigma_{uts,t}/\sigma_y$ of true ultimate tensile to yield strength, which is sensitively related to microstructural parameters, can by expressed by

$$\eta = \sigma_{uts,t}/\sigma_y = 1 + \eta_\varepsilon y. \tag{2}$$

It is related to the corresponding ratio of engineering stresses by $\eta_v = \sigma_{uts}/\sigma_y = \eta/(\exp(\varepsilon_u))$. Further, the yield strength $\sigma_y = \sigma_o + \sigma_p$ can by described by a linear superposition of matrix σ_o and precipitate obstacles hardening σ_p. Eqs. (1) and (2) demonstrate that both the work-hardening parameter η and the uniform strain decreases with increasing strength, respectively, decreasing the strength ratio $y = \Delta\sigma_{\varepsilon,m}/\sigma_y$ and the maximum strain hardening. For a given yield strength these increase by enhanced dislocation multiplication due to the presence of precipitates via $(f_v/d_p)^{1/2}$ and decrease with pronounced annihilation by high R_m values. For particle hardening dominant, $\sigma_y \cong \sigma_p = \beta_{or}\mu bM(f_v)^{1/2}/d_p$ via the Orowan by-pass process with the strength coefficient $\beta_{or} = 1/(2\Pi)\ln\{d_p[(\Pi/6f_v)]^{1/2}/b\}$ then parameter y reduces to a simpler form $y = 2(\alpha/\beta_{or})M(d_p/R)^{1/2}$. It clearly demonstrates that the work-hardening ratio η increases with increasing particle size $(d_p)^{1/2}$ more strongly at low $R(T,\dot{\varepsilon})$ values, and therefore at low temperatures and high strain rates $\dot{\varepsilon}$. Uniform strain, otherwise for the same condition and additional high yield strength increases linearly with increasing particle size according to $\varepsilon_u \sim (\alpha/\beta_{or})^2 Md_p/b$. For high y and R_m values as applicable for strong particle hardening, Eq. (2) reduces to the lower bound $\eta = 1 + (R_m/(1+R_m))y$. Thus, η increases linearly with increasing $y = \Delta\sigma_{\varepsilon,m}/\sigma_y$ and decreases with increasing R_m. At a very low strain hardening, $y < 0.1$ and R_m values Eqs. (1) and (2) reduce to $\eta = 1 + R_m y^2$ and the uniform strain to $\varepsilon_u \cong R_m y^2/2$ which correlates then with ratio η by $\eta \geqslant 1 + 2\varepsilon_u$. Thus, both work-hardening ratio η and uniform strain become independent of annihilation coefficient R_m and degrade via η, $\varepsilon_u \sim \sigma_y^{-2}$ strongly with increasing yield strength.

Ductile fracture in steels is caused by nucleation of pores and ductile microcracks at inhomogeinities which coalesce by strain-induced growth with possible contributions from local shearing. Taking into account the stress-induced ductile fracture appearance [2] and the work-hardening with the model described, the strength dependence of true fracture strain $\varepsilon_f = -\ln(1-Z)$ can be expressed by

$$\varepsilon_f = -[1/(2R_m)]\ln\{1-[(\sigma_{f,d}-\sigma_y)/\Delta\sigma_{\varepsilon,m}]^2\}, \tag{3}$$

where Z is the reduction in area at fracture. It depends on the ductile fracture stress $\sigma_{f,d}$, the maximum strain hardening $\Delta\sigma_{\varepsilon,m}$ and additionally on the annihilation coefficient R_m. Fracture strain loss is enhanced by both a reduction in ductile fracture stress and pronounced work-hardening due to the presence of a higher volume fraction f_v of small precipitates, and is stronger at lower temperatures and higher strain rates with reduced R_m values. For the reduction in area at fracture, the relation $Z = 1 - [1-\eta_\varepsilon^2]^{(1/2Rm)}$ is obtained with $\eta_\varepsilon = (\sigma_{f,d}-\sigma_y)/\Delta\sigma_{\varepsilon,m}$. At higher strengths, Eq. (3) reduces to the asymptotic lower bound $\varepsilon_f \cong \eta_\varepsilon^2/(2R_m)$ which corresponds to $Z \geqslant \{1-\exp[-\eta_\varepsilon^2/(2R_m)]\}$. This indicates a hyperbolic strength dependence $\varepsilon_f(\sigma_y)$ which becomes independent of annihilation distance R, test temperature and strain rate $\dot{\varepsilon}$. For this, the ductility ε_f decreases approximately linearly with increasing σ_y^2. The slope $S_1 = -1/(4R_m\Delta\sigma_{\varepsilon,m}^2)$ of plots ε_f vs. σ_y^2 at $\sigma_y = \sigma_{f,d}$ becomes independent of R and can be used to estimate the ductile fracture stress by extrapolation. For dominant particle hardening, the fracture strain is reduced with increasing volume fraction f_v and decreasing particle size d_p and is more pronounced at higher σ_p/σ_o ratios.

As shown by experimental observations on certain 7–12Cr steels [3], the ductile upper shelf energy (USE) of Charpy tests correlates approximately linearly with tensile fracture strain ε_f particularly at higher USE and ε_f values. Taking into account such relations, Eq. (3) is applicable to approximate strength and work-hardening effects upon the absorbed ductile energy USE. The relative increase of ductile-to-brittle transition temperature DBTT by athermal strengthening due to incoherent precipitates/particles σ_p can approximated by $V = \Delta\text{DBTT}/\text{DBTT}_0 = (K_d/P)(\sigma_p + \Delta\sigma_f^*)$ [4], where $\Delta\sigma_f^*$ is the combined change of dynamic fracture stress due to the presence of particles, P the maximum thermal

strength (Peierls stress) at $T = 0$ K and $DBTT_0$ the corresponding value for the material without particles. For 7–9CrWVNb steels, strengthened by irradiation defects about a coefficient of $K_d/P = 3.03 \times 10^{-3}$ MPa^{-1} is obtained for irradiation temperatures equal to test temperatures of 250–300 °C.

3. Comparison of experimental results with model predictions

Fig. 1 shows the yield strength $\sigma_y(T_T)$ dependence at $T_T = RT$ to 650 °C of the total elongation ε_R for 7–9CrWVTa steels like Opt.IVc-0 ppm B, F82H-30 ppm B, the 11Cr1MoVNb steel MANET-I-85 ppm B with 0.1–0.14 wt% carbon and the high nitrogen (0.16 wt%) bainitic 10Cr1.8MoVSiMnNiNb(0.05 wt% C, 110 ppm B) steel [5]. Additionally, this dependence for the oxide-dispersion-strengthened ODS-Eurofer'97 (9Cr1W0.2 V0.15Ta–0.3 wt% Y_2O_3) [6] steel with 0.12 wt% C and 0.02 wt% N is also shown in Fig. 1. Generally, a very

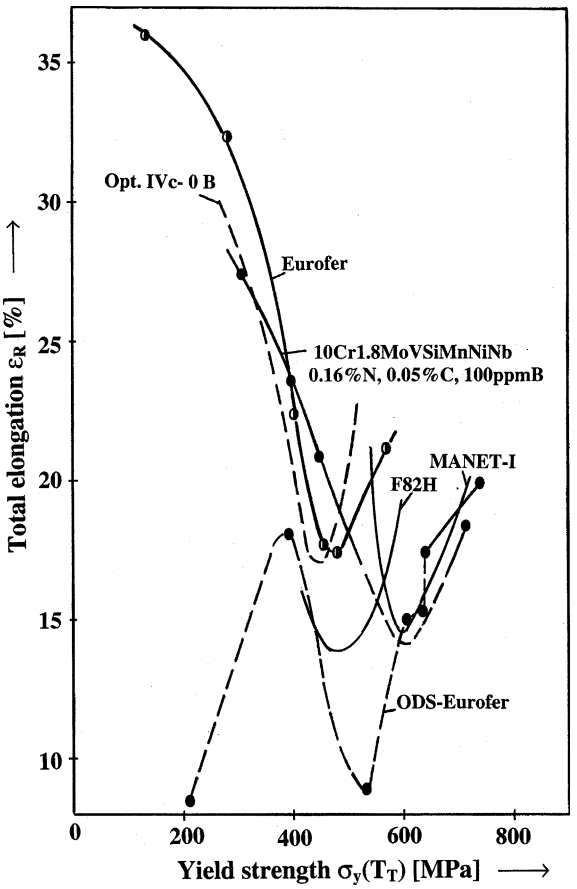

Fig. 1. The yield strength dependence of tensile elongation ε_R vs. $\sigma_y(T_T)$, $T_T = RT - 650$ °C, for various carbon and nitrogen containing martensitic 7–12Cr steels and ODS-Eurofer'97.

sharp ductility minimum appears around test temperatures of $T_T \approx 300$ °C for all martensitic and bainitic steels where dynamic strain ageing occurs due to the interaction of glide dislocations with interstitials such as carbon and nitrogen atoms. The ductility minimum tends to weakly decrease with pronounced strengthening due to increasing alloying (Cr, Mo, W, N, C) but is independent of boron content as expected if solute boron occupies interstitial sites within the matrix. Thus, it seems that boron interacts with solutes such as C and N atoms and vacancies forming small clusters as indicated by other experiments. Besides alloying content no basic differences exist between 7–9CrWVTa and 10–12CrMoVNb steels. With neutron irradiation (HFR) to low displacement damage $\leqslant 1$ dpa, the ductility minimum $\varepsilon_{R,min}$ strongly decreases for all B-doped 7–9CrWVTa and conventional 10–12CrMoVNb steels and is more pronounced at irradiation temperatures equal to test temperatures of around $T_I = T_T \approx 300$ °C due to a marked decrease in the ductile fracture stress [4]. This results from He-bubble/cluster formation at coarser $M_{23}(B, C)_6$ borocarbide interfaces which gives rise to lattice constant differences and interfacial stresses (through the ^{4}He, ^{7}Li generation via the $^{10}B^7Li(n,\alpha)$-transmutation) promoting ductile pore microcrack formation. Ductility decreases with increasing He(B, ^{7}Li)-content formed locally around and within $M_{23}(B, C)_6$-borocarbides. High nitrogen (0.17% N, 0.05% C) and also high carbon martensitic steels similar to the ODS-Eurofer'97 within the homogeneous flow region at lower temperatures $T_T = RT$ to 250 °C show similar ductility behaviour due to the same strength mechanism via the Orowan process and similar particle sizes of 10–40 nm. However, at higher temperatures of 350–600 °C, the ODS-Eurofer'97 compared to Eurofer'97 steel shows a strong reduction in work-hardening and uniform strain due to flow localization obviously induced by a inhomogeneous distribution of oxide dispersions which distinctly reduces ductile fracture stress.

Fig. 2 shows the temperature dependence of the work-hardening parameter η_v for various carbon (≈0.1% C) containing martensitic steels (Eurofer'97, MANET-I), the higher carbon (0.24–0.27% C) but low-alloyed 1.4MnMoNiSi steels [7] with 11–17 ppm B, 15–37 ppm N and also the high nitrogen containing bainitic 10Cr1Mo0.26V0.26Si0.16Mn0.11Ni0.05Nb-(0.05% C, 0.16% N, 110 ppm B) [5] and martensitic 10.4Cr1.8Mo0.2V0.07Nb0.1Si(NF616)–(0.06–0.15)% N, 0.1% C [8] steels with their modifications N7(N/C = 3.65, 12 ppm B, 0.11% N) and N6(N/C = 1.29, 49 ppm B, 0.143% N) together with ODS-Eurofer'97. A minimum in work-hardening η_v and uniform ductility generally appears around 600 °C at the onset of strong static dislocation recovery due to a change in the dislocation structure. Above 600 °C by the combined action of recovery-induced softening and diminishing dislocation

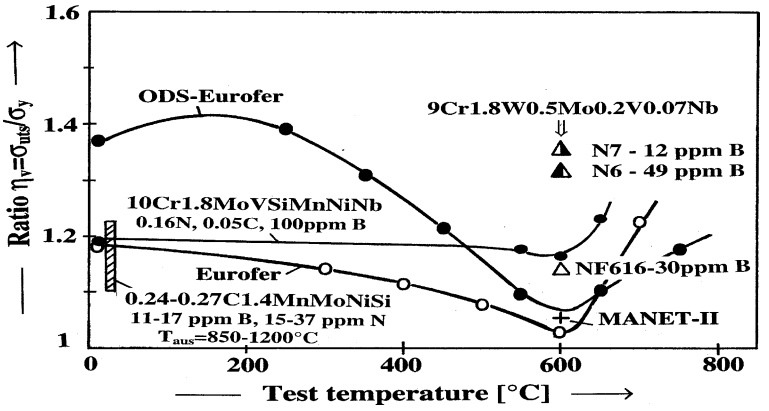

Fig. 2. Temperature dependence of work-hardening parameter η_v of N and C-strengthened martensitic $\leqslant 12$ Cr steels and Y_2O_3-oxide particle strengthened ODS-Eurofer'97.

multiplication from increasing glide distances Λ, work-hardening and uniform ductility increases. Below 600 °C, η_v increases due to enhanced multiplication (decrease in Λ) and reduced dynamic recovery with low R_m values which dominates over the strength increase. With nitrogen alloying more effective than carbon alloying, the work-hardening minimum is increased by replacement of $M_{23}(C, B)_6$ and MC precipitates by finer Cr_2N and MN nitrides with increasing particle structure ratio f_v/d_p. Strengthening by Y_2O_3-particles in ODS-Eurofer'97 increases the 600 °C work-hardening minimum weakly but stronger work-hardening occurs at lower temperatures. As shown by a plot of the ratio η_v vs. (N + C)-content, work-hardening of 7–12Cr steels at 600 °C strongly increases from $\eta_v = 1.02$ at $C + N \cong 0.12$ to about 1.35 for $C + N \cong 0.22$ as expected due to pronounced precipitate formation during cooling and tempering. The strong scatter in dependence, however, indicates additional effects due to variations in particle strengthening and structure factor f_v/d_p. High nitrogen alloying causes finer nitride precipitation in the matrix and might also induce local ordering which acts as strong barriers against dislocation motion. In unstabilized ferritic steels, the effect of carbon addition on increase of strength and work-hardening is only weak.

Fig. 3 shows the yield strength dependence of the work-hardening parameter η_v at 20 °C for low-alloyed ferritic 0.16–0.29C–MnSi(V) steel [7], various martensitic 7–9CrWVTa steels together with Y_2O_3 dispersion-strengthened ferritic–martensitic 9–13Cr steels such as ODS-Eurofer'97, the Ti alloyed 12Cr2.2Ti1.4Mo–0.38 wt% Y_2O_3(0.16% N, 0.02% C) (K2) [9] and 13Cr1.5Ti 0.6Mo–0.39 wt% Y_2O_3(0.015% N, 0.011% C) (K5) [9]

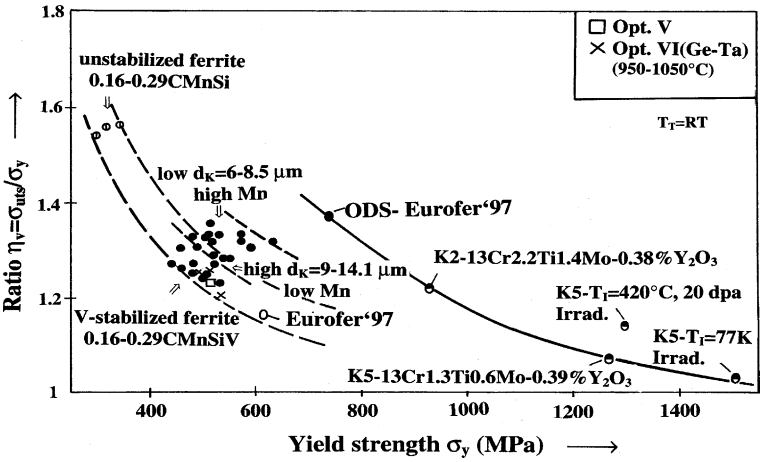

Fig. 3. Effect of Y_2O_3-oxide particle strengthening and grain size on the strength dependence of work-hardening parameter η_v for various ferritic–martensitic and ODS-(9–13)Cr steels.

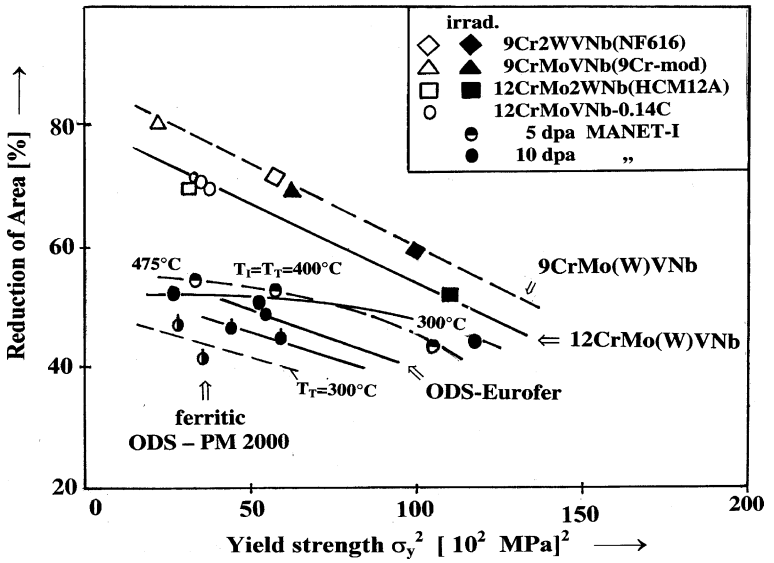

Fig. 4. The yield strength dependence of fracture strain Z vs. σ_y^2 for 9–12CrMo(W)VNb steels irradiated at 300–475 °C to 2.5–10 dpa and for ODS-Eurofer'97 and ODS-PM2000 steels at $T_T = RT$.

steel unirradiated and irradiated at $T_I = 420$ °C to 20 dpa as well as at $T_I = 77$ K to a low dose. In accordance with model predictions (Eq. (2)), the ratio η_v strongly decreases with increasing yield strength. It does not disappear at higher strengths as observed at higher temperatures of $T_T = T_I = 300$ °C for all HFR-irradiated 7–9CrW(Ge)VTa steels above about $\sigma_y \cong 800$ MPa [2]. For the low-alloyed ferritic steels, work-hardening is increased with decreasing grain size from 9–14.1 μm to 6–8.5 μm caused by V-stabilization. The 7–9CrWVTa steels with 0.1–0.12% C and lath-pocket sizes of 3–6 μm and an individual lath width of ≈0.3 μm as in Eurofer'97 show at similar yield strengths a comparable work-hardening as the larger grain sized 9–14.1 μm, low-alloyed higher carbon containing ferritic steels. This demonstrates that dislocation glide distances are less than grain and/or lath pocket sizes in ferritic and martensitic structures and dislocation multiplication by enhanced precipitation due to higher C and Mn alloying is further increased. In ODS-(9–13)Cr steels with 0.3–0.39 wt% Y_2O_3, the work-hardening ratio η_v is strongly increased by refinement of oxide particles to ≈8 nm and increase of ratio f_v/d_p which shifts the η_v vs. σ_y curve about 350 MPa higher in yield strength arising from the increase of maximum strain hardening $\Delta\sigma_{\varepsilon,m}$. A measurable work-hardening and uniform ductility remains in this particle strengthened steels up to high yield strength levels of about 1500 MPa because ductile fracture stresses are higher. By irradiation at 420 °C to 20 dpa for the K5-ODS-steel strength and η_v weakly increase as might be expected from additional irradiation-induced precipitation.

The fracture strain of Nb-stabilized 9–12Cr steels, in accordance with predictions from Eq. (3) for high strengths, is reduced with increasing yield strength as shown in Fig. 4 in the plot of Z vs. σ_y^2. For 12Cr steels like HCM12A [3] unirradiated and irradiated at 300 °C to 2.5 dpa in the HFR and unirradiated MANET-I at $T_T = RT$, the ductilities Z are a little lower compared to that of 9Cr steels 9Cr-mod and NF616 [3]. However, irradiation of the 85 appm B containing MANET-I at $T_I = T_T = 300$–475 °C to 5–10 dpa strongly reduces fracture strain especially at the higher temperature 475 °C due do a reduction of the ductile fracture stress. Whereas at 475 °C, this occurs due to an irradiation-enhanced ageing [4] with coarsening of $M_{23}(B, C)_6$ borocarbides, at lower irradiation temperatures of around 300 °C it is caused by He-bubble formation at the interfaces of the $M_{23}(B, C)_6$ [4]. Particle strengthening of ODS-Eurofer'97 and the ferritic 20CrAlTiC ODS-steel PM 2000 [10] with 0.5 wt% Y_2O_3 strongly reduces fracture strain to around similar levels as irradiated MANET-I. This ductility reduction is caused by enhanced work-hardening possibly assisted by a reduction of ductile fracture stress. As indicated for PM 2000, the fracture strain is further reduced at the somewhat higher $T_T = 300$ °C due to enhanced localized deformation reducing the ductile fracture stress.

Fig. 5 demonstrates the effect of strengthening due to irradiation and Y_2O_3-oxide particles on the relationship between shift of dynamic embrittlement $V = \Delta DBTT/DBTT_0$ and ductile upper shelf energy $U = \Delta USE/USE_0$ ($DBTT_0$ and USE_0 for unirradiated or particle free steels) for 7–9CrW(Ge)VTa steels together with ODS-

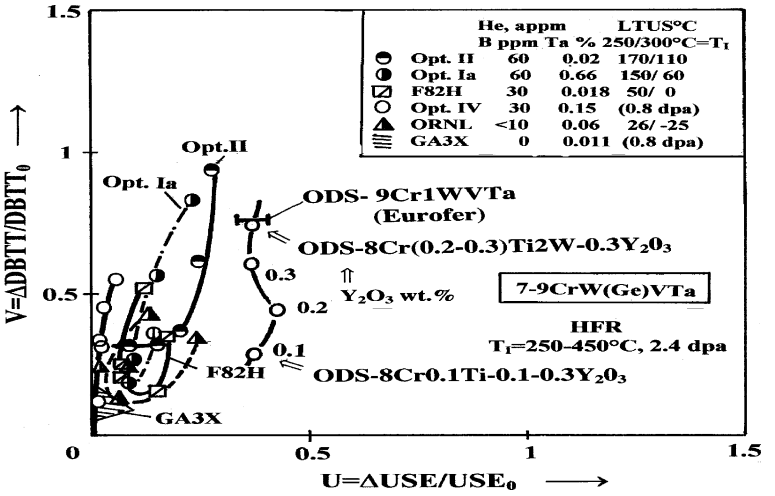

Fig. 5. Comparison of the correlation between DBTT and USE shifts for irradiation-strengthened 7–9CrW(Ge)VTa steels ($T_I = 250$, 300 °C, 2.4 dpa) and oxide particle strengthened ODS-(9–13)Cr steels.

Eurofer'97 and certain ODS-8Cr(0.1–0.3)Ti(0–2)W–(0.1–0.3) wt% Y_2O_3 [11] steels. From irradiation strengthening ($T_I = 250$–450 °C at 2 dpa in HFR) a distincly lower shift $U \leqslant 0.25$ compared to embrittlement $V \leqslant 0.9$ occurs which increases with increasing strengthening at lower irradiation temperatures. For particle strengthened ODS-Eurofer'97 and ODS-8Cr(0.2–0.3)Ti2W–0.3 wt% Y_2O_3 steels a comparable embrittlement shift $V \cong 0.29$–0.75 is observed which increases with increasing Y_2O_3 content. But a strong ductile energy reduction $U \cong 0.35$–0.4, in contrast to irradiated 7–9CrWVTa steels, appears for low 0.1 wt% Y_2O_3 contents. This drop of USE arises from a marked reduction in ductile fracture stress due to localized flow which acts stronger above 200 °C within the region of low strain rate sensitivities of strength. The strength-induced embrittlement shift $\approx 2.8 \times 10^{-3}$ V/MPa^{-1} ($T_T = RT$) in ODS-Eurofer'97 is comparable to that observed due to irradiation hardening of $\cong 3.03 \times 10^{-3}$ V/MPa^{-1} for 7–9CrWVTa steels at $T_I = 250/300$ °C which is somewhat larger than $\cong 2.42 \times 10^{-3}$ V/MPa^{-1} observed for 12Cr steels.

4. Conclusions

From the analysis of results of work-hardening, ductility and impact behaviour of carbon and nitrogen martensitic 7–12Cr, as well as ODS-(9–13) Cr steels, the following conclusions can be drawn.

Work-hardening uniform and fracture strain generally decrease with increasing yield strength in accordance with model predictions. Uniform strain does not disappear at 20 °C in the high strength ODS-steels below 1500 MPa as observed for irradiation-strengthened 7–9CrW(Ge)V Ta steels at higher $T_T = T_I = 300$ °C.

Pronounced precipitation (from increasing N and C contents) or fine Y_2O_3-dispersions in ODS-(9–13)Cr steels strongly increase work-hardening and uniform ductility but decrease fracture strain and USE of impact tests. The later is additionally enhanced by localized flow which distinctly decreases ductile fracture stress.

Minima of work-hardening and uniform strain appear for carbon and high nitrogen martensitic 7–12Cr steels around 600 °C at the onset of strong dislocation recovery and for total elongation and fracture strain at ≈300 °C, where dynamic strain ageing results. The later weakly decreases with increasing strengthening due to alloying independent of boron content.

The strength-induced increase of ductile-to-brittle transition temperature of ODS-steels is comparable to that observed due to irradiation strengthening.

For dominant particle strengthening, the work-hardening according to model predictions increases with particle size by $\eta \sim (d_p/R)^{1/2}$ and the uniform strain varies linearly with $\varepsilon_u \sim d_p$ at high strength.

References

[1] U.F. Kocks, J. Eng. Mater. Tech. (ASME H) 98 (1976) 76.
[2] D. Preininger, FZKA 5701 (1996).
[3] M.G. Horsten, E.V. van Osch, D.S. Gelles, M.L. Hamilton, Effects of radiation on materials, in: M.L. Hamilton, A.-S. Kumar, S.T. Rosinski, M.L. Grossbeck (Eds.), 19th International Symposium ASTM STP 1366, West Conshohocken, PA, 1999, p. 134.
[4] D. Preininger, in: Proceedings of Materials Week 2000, 25/28.9, Munich, 2001. Available from <httpwww.materials-week.org>.
[5] H. Kanbach, A. Rukwied, in: Proceedings of High Nitrogen Steels HNS'90, Aachen, Germany, 10/12.1990, p. 143.

[6] R. Lindau, M. Schirra, Workshop, 27/28.11, Brasimore, Italy, 2000.
[7] M. Eisaa, Steel Res. 69 (1998) 438.
[8] P. Ernst et al., in: Proceedings of High Nitrogen Steels HNS'90, Aachen, Germany, 10/12.1990, p. 99.
[9] V.V. Sagardze, V.I. Shalaev, V.L. Arbuzov, B.N. Goshchitskii, Y. Tian, W. Qun, S. Jiguang, J. Nucl. Mater. 295 (2001) 265.
[10] G. Filacchoni, ODS-Workshop, Karlsruhe, 2001.
[11] JAERI, Workshop, Material Assessment Meeting, 2001.